JOC The Journal of Organic Chemistry

Article

pubs.acs.org/joc

Nitro-Substituted 4-[(Phenylmethylene)imino]phenolates: Solvatochromism and Their Use as Solvatochromic Switches and as Probes for the Investigation of Preferential Solvation in Solvent Mixtures

Leandro G. Nandi, Felipe Facin, Vanderléia G. Marini, Lizandra M. Zimmermann, Luciano A. Giusti, Robson da Silva, Giovanni F. Caramori, and Vanderlei G. Machado*

Departamento de Química, Universidade Federal de Santa Catarina, UFSC, CP 476, Florianópolis, Santa Catarina 88040-900, Brazil

Supporting Information

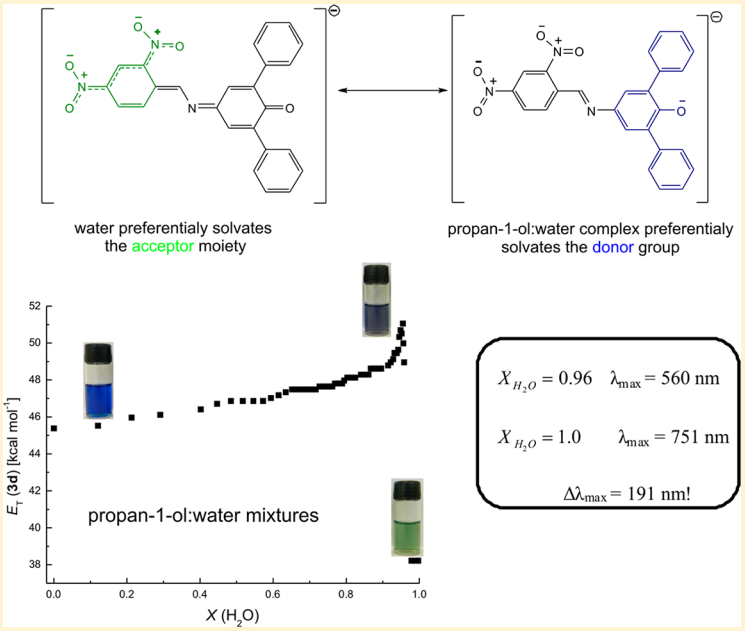

ABSTRACT: Four 4-[[(4-nitrophenyl)methylene]imino]phenols (**2a−d**) were synthesized. After deprotonation in solution, they formed the solvatochromic phenolates **3a−d**, which revealed a reversal in solvatochromism. Their UV−vis spectroscopic behavior was explained on the basis of the interaction of the dyes with the medium through combined effects, such as nonspecific solute−solvent interactions and hydrogen bonding between the solvents and the nitro and phenolate groups. Dyes **3a−c** were used as probes to investigate binary solvent mixtures, and the synergistic behavior observed was attributed to solvent−solvent and solute−solvent interactions. A very unusual UV−vis spectroscopic behavior occurred with dye **3d**, which has in its molecular structure two nitro substituents as acceptor groups and two phenyl groups on the phenolate moiety. In alcohol/water mixtures, the E_T(**3d**) values increase from pure alcohol (methanol, ethanol, and propan-2-ol) until the addition of up to 80−96% water. Subsequently, the addition of a small amount of water causes a very sharp reduction in the E_T(**3d**) value (for methanol, this corresponds to a bathochromic shift from 543 to 732 nm). This represents the first example of a solvatochromic switch triggered by a subtle change in the polarity of the medium, the color of the solutions being easily reversed by adding small amounts of the required cosolvent.

INTRODUCTION

Various physicochemical events, such as the rate, course, and position of the equilibrium of processes and the spectroscopic data of compounds, are influenced by the solvents in which they are carried out.[1−5] These solvent effects are commonly interpreted as arising from changes in the polarity, a general term that is related to the overall solvating capability of the medium.[1,5] The solvent polarity causes changes in the absorption and/or emission spectra of many organic dyes.[1,2] This phenomenon is known as solvatochromism, and the spectral changes can be potentially used in the investigation of

Received: September 10, 2012
Published: October 22, 2012

solvent properties.[1,2,5] Many solvatochromic probes are known, the most popular example being Reichardt's betaine dye, 2,6-diphenyl-4-(2,4,6-triphenylpyridinium-1-yl)phenolate (**1**). The maximum absorption of **1** in different solvents is the basis for the very commonly employed $E_T(30)$ polarity scale.[1,2,5] The perichromic properties of this compound and others with related molecular structure have allowed their use in a large number of applications.[1,5,6]

In the research carried out applying solvatochromic probes to understand medium effects, much attention has been given to the chemistry of solvent mixtures.[7−36] The behavior of solutes in these systems is more complex than in pure solvents due to the fact that in many cases preferential solvation (PS) occurs, leading to a solute microenvironment having more of one solvent than the other, in comparison to the bulk composition. Therefore, this is a very important subject in terms of analyzing kinetic, spectroscopic, and equilibrium data in solution. It is also important to observe that mixed solvents are used in many industrial applications.[8,37]

The consideration that structurally different probes should be able to detect different aspects of the physical chemistry of pure and mixed solvents is important for the design of different systems with the potential to act as solvatochromic compounds. In this paper, we describe the synthesis of a series of 4-[[(4-nitrophenyl)methylene]imino]phenols (**2a−d**) and the behavior of their conjugated bases (**3a−d**) as solvatochromic probes. The motivation for this study came from the results of our previous research involving compounds able to act as chromogenic chemosensors for anions in solution. We studied 4-[[(4-nitrophenyl)methylene]imino]-2,6-diphenylphenol (**2c**) in acetonitrile and in acetonitrile/water mixtures[38] and discovered that this compound, when deprotonated, colors solutions and that the color changes depend on the percentage of water in the medium.[38] Thus, herein, we describe the UV−vis spectral behavior of **3a−d** in pure solvents and potential applications of these compounds as probes to investigate binary solvent mixtures and as solvatochromic switches. The data obtained are discussed on the basis of dye−solvent, dye−dye, and solvent−solvent interactions.

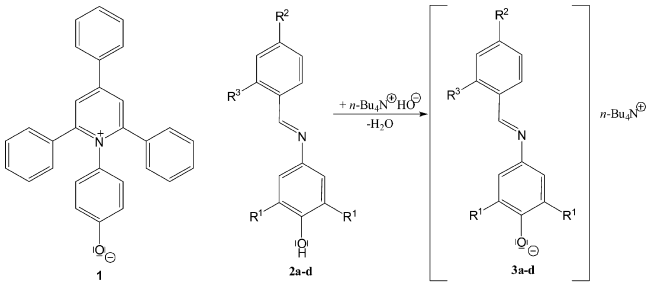

2, 3	a	b	c	d
R^1	H	H	C_6H_5	C_6H_5
R^2	NO_2	NO_2	NO_2	NO_2
R^3	H	NO_2	H	NO_2

RESULTS AND DISCUSSION

Synthesis of the Dyes and Influence of Solvents on Their UV−vis Spectra. Compounds **2a−d** were synthesized by condensation of the corresponding 4-aminophenols with 4-nitrobenzaldehyde or 2,4-dinitrobenzaldehyde in the presence of a small amount of acetic acid (Scheme 1). The compounds were purified by recrystallization, and the characterizations showed that their purity was adequate for the spectroscopic studies.

Scheme 1. Preparation of Compounds 2a−d

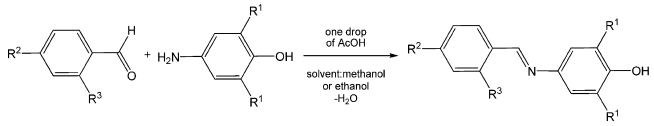

Compounds **2a−d** are almost colorless in solution, but their solutions turn colored when they are deprotonated to give **3a−d**. Importantly, as can be observed in Figure 1, **3a−d** are

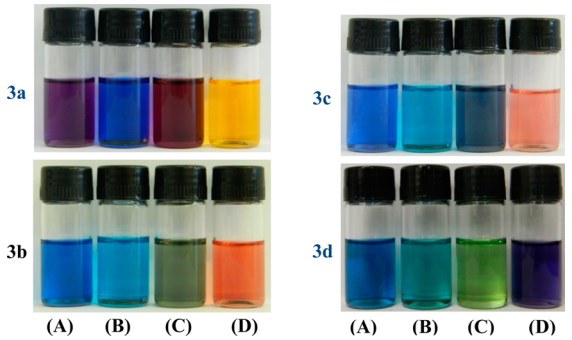

Figure 1. Solutions of **3a−d** in ethyl acetate (A), DMA (B), acetophenone (C), and methanol (D).

solvatochromic, exhibiting a very large range of colors in solution. Figure 2 shows the UV−vis spectra for **3a−d** in selected solvents, which reinforces the solvatochromic behavior of these species. It can be observed that, for instance, the solvatochromic band of **3a** has a λ_{max} at 446 nm in methanol (ε_{max} = 1.80 × 10^4 L mol^{-1} cm^{-1}), which is bathochromically shifted to 508 nm in 1,2-dichloroethane (ε_{max} = 1.42 × 10^4 L mol^{-1} cm^{-1}): $\Delta\lambda_{max}$ = +62 nm. The deprotonation of compounds **2a−d** was performed using tetra-*n*-butylammonium hydroxide. The presence of the bulky ammonium ion inhibits the formation of ion pairs with the anion in solution. This was confirmed by the fact that, with the addition of tetra-*n*-butylammonium tetrafluoroborate at a concentration of up to 2.8 mol ×10^{-4} L $^{-1}$ to the solutions of **3a−d** (5.0 × 10^{-5} mol L^{-1}) in methanol, the UV−vis spectrum of the dyes remained unaltered, while only a very small decrease (4%) in the maximum absorbance value was detected in ethyl acetate. The solvatochromic band observed in the UV−vis spectra of **3a−d** is due to a $\pi-\pi^*$ transition, of an intramolecular charge-transfer nature, from the phenolate donor moiety to the nitrophenyl acceptor group, which is reinforced by the molecular structures of **3a−d**, optimized by applying density functional theory, DFT, which exhibit a high planarity in comparison with the molecular structures of **2a−d**. In addition, the frontier molecular orbitals in **3a−d** are more delocalized through the π-aromatic system than those in **2a−d**. As an example, the structure of **3d** is planar, whereas that of **2d** is twisted. According to Figure 3, the HOMO electron density in **2d** is mainly located in the phenolate donor moiety, whereas the LUMO electron density is mainly located on the nitrophenyl acceptor group, indicating the donor and acceptor moieties. In the case of **3d** the situation is different. Both HOMO and LUMO electron densities are

dx.doi.org/10.1021/jo301890r | J. Org. Chem. 2012, 77, 10668−10679

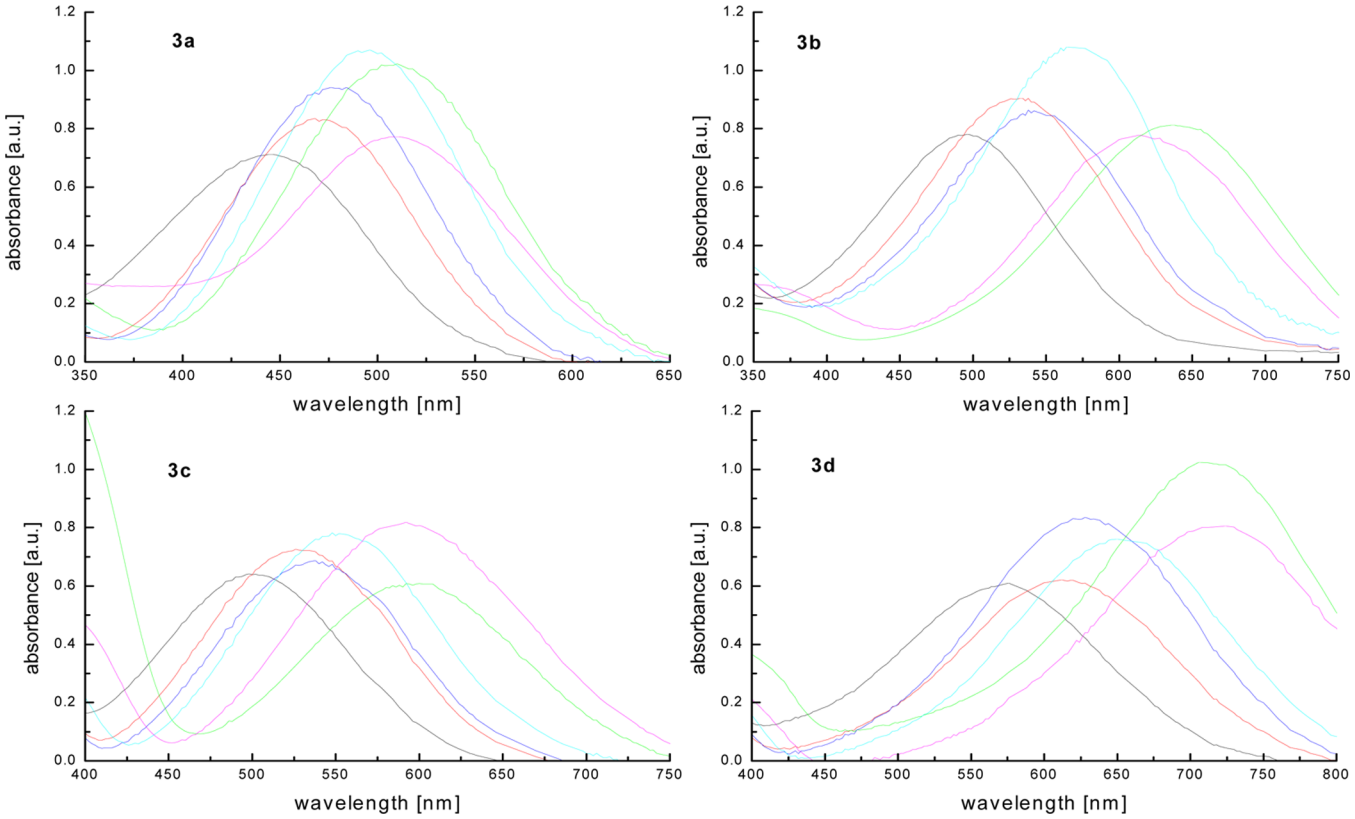

Figure 2. UV−vis spectra of **3a−d**, measured in methanol (gray), ethanol (red), propan-1-ol (blue), octan-1-ol (blue-green), ethyl acetate (green), and 1,2-dichloroethane (pink) at 25 °C.

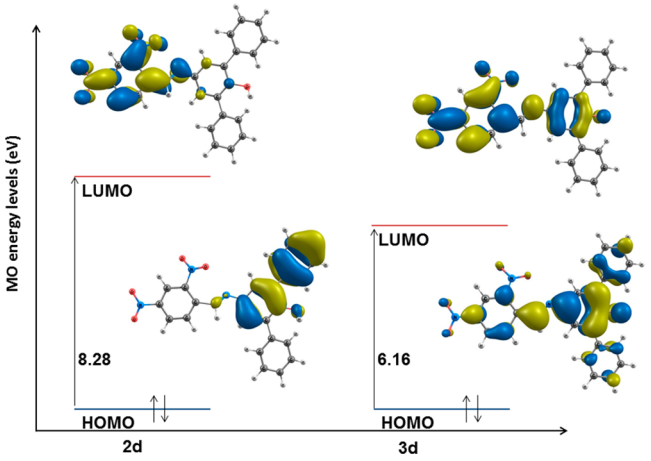

Figure 3. Frontier orbitals of compounds **2d** and **3d**.

delocalized through the phenolate and nitrophenyl moieties, exhibiting an energy gap which is 2.00 eV smaller than that in **2d**. These findings (as expected) lead to the characteristic color of dyes **3a−d** when excited.

The UV−vis spectra of these compounds were measured in 23 solvents. The absorbance maxima in each spectrum were obtained with a precision of ±0.5 nm, and the reproducibility of the λ_{max} values was verified by the determination of five spectra for each dye in each pure solvent. All data were transformed into E_T(dye) values, given in kilocalories per mole with a precision of ±0.1 kcal mol^{-1}, which are shown in Table 1. Table 1 also shows, for the solvents used in this study, the Reichardt polarity scale $E_T(30)$[1,5,36] and the Kamlet−Taft α (solvent hydrogen bond donor acidity), β (solvent hydrogen bond acceptor basicity), and π^* (solvent dipolarity/polarizability) parameters,[39,40] which are commonly used to describe solvent polarity and solvent hydrogen-bonding properties. The data show very large shifts of the solvatochromic absorption band of the dyes depending on the polarity of the medium. For dye **3a**, a change in the medium from water to *N*,*N*-dimethylacetamide (DMA) leads to a shift of $\Delta\lambda_{max}$ = 149.5 nm (λ_{max}(DMA) = 580.0 nm and λ_{max}(water) = 430.5 nm), while for dyes **3b** and **3c** the $\Delta\lambda_{max}$ values obtained are 244.0 nm (λ_{max}(DMA) = 708.0 nm and λ_{max}(water) = 464.0 nm) and 232.0 nm (λ_{max}(DMA) = 654.0 nm and λ_{max}(water) = 422.0 nm), respectively. In comparison, the same solvents cause a shift of $\Delta\lambda_{max}$ = 213.0 nm (λ_{max}(DMA) = 666.0 nm and λ_{max}(water) = 453.0 nm) in the solvatochromic band of pyridiniophenolate **1**. For dye **3d** the shift obtained is relatively low due to the fact that the E_T(**3d**) value obtained in water is small (see the discussion below), but its solvatochromic shift, compared with those in methanol (λ_{max} = 573.0 nm) and DMA (λ_{max} = 758.5 nm), is very significant ($\Delta\lambda_{max}$ = 185.5 nm).

Figure 4 shows plots of E_T(dye) as a function of the E_T(30) values for **3a−d** in the pure solvents. The plots for **3a−c** indicate a reversal in solvatochromism: the E_T values first decrease from water to DMA; i.e., a hypsochromic shift of the solvatochromic band of the dyes occurs with an increase in the polarity of the medium. However, for solvents with E_T(30) values below 42.9 kcal mol^{-1}, the E_T(dye) values increase until the least polar solvent studied (*n*-hexane), a bathochromic shift occurring in the solvatochromic band of the dyes when the polarity of the medium is increased. The concept of the reversal in solvatochromism has been discussed over the past four decades,[41] being observed for various solvatochromic cyanines

dx.doi.org/10.1021/jo301890r | J. Org. Chem. 2012, 77, 10668−10679

Table 1. E_T(dye) Values for Compounds 3a–d in 23 Pure Solvents at 25 °C and the Corresponding "Polarity" $E_T(30)$ and Kamlet–Taft Parameters

solvent	$E_T(30)^a$	α^b	β^b	π^{*b}	$E_T(\mathbf{3a})^c$	$E_T(\mathbf{3b})^c$	$E_T(\mathbf{3c})^c$	$E_T(\mathbf{3d})^c$
water	63.1	1.17	0.47	1.09	66.4	61.6	67.7	38.1
ethane-1,2-diol	56.3	0.90	0.52	0.92	64.4	57.6	56.9	49.1
methanol	55.4	0.98	0.66	0.60	64.1	57.7	57.3	49.9
ethanol	51.9	0.86	0.75	0.54	61.0	54.1	54.25	46.5
propan-1-ol	50.7	0.84	0.90	0.52	53.4	52.7	53.1	46.0
benzyl alcohol	50.4	0.60	0.52	0.98	59.3	52.3	52.2	45.6
butan-1-ol	49.7	0.79	0.88	0.47	59.3	51.8	53.1	44.1
propan-2-ol	48.4	0.76	0.84	0.48	58.3	49.8	51.7	43.7
octan-1-ol	48.1	0.77	0.81	0.40	58.6	49.5	51.8	43.8
decan-1-ol	47.7	0.70	0.82	0.45	58.8	49.5	52.2	44.1
butan-2-ol	47.1	0.69	0.80	0.40	56.9	48.9	49.3	43.7
acetonitrile	45.6	0.19	0.40	0.75	55.8	49.3	49.3	41.0
DMSO	45.1	0.00	0.76	1.00	49.3	47.8	44.9	44.1
2-methylpropan-2-ol	43.7	0.42	0.93	0.41	54.1	44.9	49.8	40.9
DMF	43.2	0.00	0.69	0.88	49.5	38.81	43.7	37.7
DMA	42.9	0.00	0.76	0.88	49.3	40.4	43.7	37.7
acetone	42.2	0.08	0.43	0.71	54.3	49.3	49.1	37.7
1,2-dichloroethane	41.3	0.0	0.0	0.81	56.2	46.5	48.5	39.9
dichloromethane	40.7	0.13	0.10	0.82	56.0	49.3	49.3	41.0
acetophenone	40.6	0.04	0.49	0.90	50.0	49.1	43.5	38.3
trichloromethane	39.1	0.20	0.10	0.58	57.6	48.5	49.3	41.5
ethyl acetate	38.1	0.00	0.45	0.55	56.0	44.9	47.9	40.4
n-hexane	31.0	0.0	0.0	−0.04	58.8	58.3	53.1	46.0

[a]Values obtained from the literature,[1,5] given in kilocalories per mole. [b]Values obtained from the literature.[39,40] [c]This study, values given in kilocalories per mole.

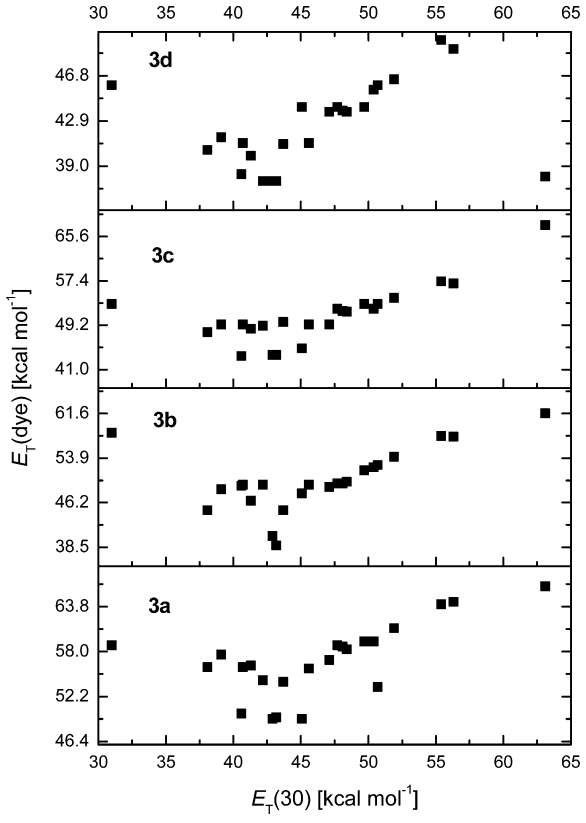

Figure 4. E_T(dye) values for **3a–d** in various solvents as a function of Reichardt's $E_T(30)$ parameter.

and merocyanines.[42−48] Although some authors have interpreted the phenomenon in terms of dye aggregation in low-polarity solvents[46,49,50] and of solvent-dependent *cis–trans* isomerization processes,[51,52] the most common explanation given is related to the different abilities of polar and nonpolar solvents to stabilize the ground and excited states of the dye. Scheme 2 shows two resonance structures for dye **3a**, one

Scheme 2. Benzenoid and Quinonoid Resonance Structures for the Anion of Dye 3a

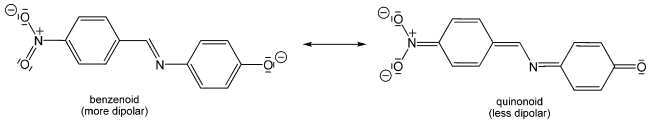

benzenoid (more dipolar) and the other quinonoid (less dipolar), both representative of the other dyes studied. More polar solvents are able to stabilize the benzenoid form, which contributes to the ground state to a greater extent than the quinonoid form, being responsible for the negative solvatochromism observed (the higher the polarity of the medium, the higher the HOMO–LUMO gap). In less polar solvents, however, the quinonoid structure makes a greater contribution to the ground state, causing the reversal in solvatochromism; i.e., on increasing the polarity of the medium, the difference between the ground and excited states is reduced. For dyes **3a–c** a roughly linear correlation between the $E_T(30)$ and E_T(dye) values for the region corresponding to the hydroxylic solvents was observed. Compound **1**, the basis for the $E_T(30)$ scale, has a phenolate donor group in its molecular structure and is therefore very susceptible to the acidity of the medium, being capable of interacting through hydrogen bonding with hydroxylic solvents.[53] Dyes **3a–d** also have a phenolate group in their molecular structure, which makes them also

dx.doi.org/10.1021/jo301890r | J. Org. Chem. 2012, 77, 10668–10679

capable of interacting with hydrogen bond donating (HBD) solvents. According to Zhao and Han,[54] a hypsochromic shift observed in the solvatochromic band of a compound with an increase in the hydrogen bond (HB) donor ability of the solvent indicates a weakening of the dye−solvent intermolecular HB in the corresponding electronic excited state. This rationalization can be applied to the spectral behavior of dyes **3a−d**. Han and co-workers have observed that intermolecular HB weakening and strengthening in the electronic excited states facilitates many nonradiative processes,[54] such as solute−solvent photoinduced electron transfer[55] and intramolecular charge transfer.[56]

However, the data show that, in the case of **3d**, the presence of two nitro groups associated with pending phenyl groups develops a fundamental role in giving the compound its unique solvatochromic properties. This dye has a very similar behavior in relation to the other dyes studied, but a comparison between methanol and water reveals that, in contrast to the behavior of the other dyes studied, a notable lack of linearity is observed, with an E_T(**3d**) value decreasing from 49.9 kcal mol^{-1} in methanol (λ_{max} = 572 nm) to 38.1 kcal mol^{-1} in water (λ_{max} = 750 nm), corresponding to a $\Delta\lambda_{max}$ of 178 nm. On the basis of studies performed with this system following the methodology proposed by El Seoud and co-workers,[46] the possibility of aggregation or *cis−trans* isomerization for **3d** in methanol and water was discarded. The data suggest that water is able to stabilize the quinonoid form of the dye through specific interactions, as shown in Scheme 3. An analysis of the α

Scheme 3. Stabilization of the Quinonoid Form of the Anion of 3d by Water

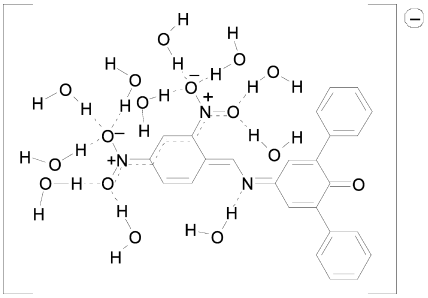

Kamlet−Taft parameter reveals a larger value for water (1.17) in comparison with methanol (0.98). In addition, considering the molecular structure of the dyes, this anomalous effect occurs only with dye **3d**, which has both two acceptor nitro substituents and two phenyl groups on the phenolate donor moiety. In principle, water would interact with both the nitro and phenolate groups through hydrogen bonding, but the data indicate that because of the molecular design of the dye, the water preferentially solvates the nitro groups, probably due to the fact that the presence of nitro groups on one side and phenyl groups on the other makes the acceptor 2,4-dinitrophenyl group more hydrophilic. These observations suggest that dye **3d** has the potential to be used as a solvatochromic switch (see below).

Preferential Solvation (PS) of the Dyes in the Mixed Solvents. Dyes **3a−d** can be used to investigate binary solvent mixtures. To study the PS of the dyes, the two-step solvent-exchange model shown below was used, taken from a study by Skwierczynski and Connors:[57]

$$\text{dye}(S_1)_2 + 2S_2 \rightleftarrows \text{dye}(S_2)_2 + 2S_1$$

$$\text{dye}(S_1)_2 + S_2 \rightleftarrows \text{dye}(S_{12})_2 + S_1$$

This model has been used successfully to describe the PS of dye **1**[27,58−60] and other solvatochromic probes[13−15,17,19−21,23,25,27,28,30,31] in various binary solvent mixtures. S_1 and S_2 represent the two solvents in the mixture, and the subscript 2 refers to the more polar component. The interaction of S_1 and S_2 by means of hydrogen bonding forms a common structure, S_{12}. Solvation of the probe by S_1, S_2, and S_{12} is represented by dye$(S_1)_2$, dye$(S_2)_2$, and dye$(S_{12})_2$, respectively. The two solvent-exchange processes shown above are defined by $f_{2/1}$ and $f_{12/1}$, which are two PS parameters that measure the tendency of the probe to be solvated by S_2 and S_{12} in relation to solvent S_1, according to

$$f_{2/1} = (X_2^{L}/X_1^{L})/(X_2/X_1)^2 \quad (1)$$

$$f_{12/1} = (X_{12}^{L}/X_1^{L})/(X_2/X_1) \quad (2)$$

where X_1^{L}, X_2^{L}, and X_{12}^{L} are the S_1, S_2, and S_{12} mole fractions, respectively, in the microenvironment of the dye. X_1 and X_2 are the mole fractions of S_1 and S_2 in the bulk binary mixture. The E_T(dye) for a given mixture is equal to the average of the E_T(dye) values of S_1, S_2, and S_{12} in the cybotactic region of the dye, resulting in the following equation:

$$E_T(\text{dye}) = X_1^{L}E_T(\text{dye})_1 + X_2^{L}E_T(\text{dye})_2 + X_{12}^{L}E_T(\text{dye})_{12} \quad (3)$$

Substituting eqs 1 and 2 into eq 3 leads to the following equation, which relates E_T(dye) in the mixed system to the E_T(dye) values of each pure component:[58−60]

$$E_T(\text{dye}) = \frac{E_T(\text{dye})_1(1-X_2)^2 + E_T(\text{dye})_2 f_{2/1}X_2^2 + E_T(\text{dye})_{12}f_{12/1}(1-X_2)X_2}{(1-X_2)^2 + f_{2/1}X_2^2 + f_{12/1}(1-X_2)X_2} \quad (4)$$

Plots of the E_T(dye) values for dyes **3a−c** as a function of X_2 (water mole fraction) are presented in Figure 5, and nonlinear regression fits of the experimental data were performed using eq 4. The results are displayed in Table 2 and show a standard deviation (SD) of $<4.4 \times 10^{-3}$ for all binary solvent mixtures studied. Table 2 also shows the PS parameter $f_{12/2}$, which is a measure of the tendency of the probe to be preferentially solvated by the solvent S_{12} in comparison with S_2. This parameter is calculated through the expression $f_{12/2} = f_{12/1}/f_{2/1}$. The calculated E_T(dye) values in Table 2 for the pure solvents are in good agreement with the experimental values shown in Table 1.

Figure 5 shows plots of the E_T(dye) values of compounds **3a−c** as a function of the water mole fraction for its mixtures with methanol. A very strong synergistic effect is observed for these mixtures, and the E_T values are lower than those for the pure solvents. Synergism is often observed in the analysis of solvatochromic probes in solvent mixtures,[13,14,17,20,27,28,58−63] and this term was first employed by Reichardt and co-workers.[61] It occurs due to the presence of a hydrogen bond accepting (HBA) solvent and a HBD partner in the binary solvent mixture, which form 1:1 S_{12} complexes through hydrogen bonding. Data from the literature have demonstrated that these species solvate the solute in different manners. Compound **1**[27,58,59,61] and Brooker's merocyanine[14,17,27] are

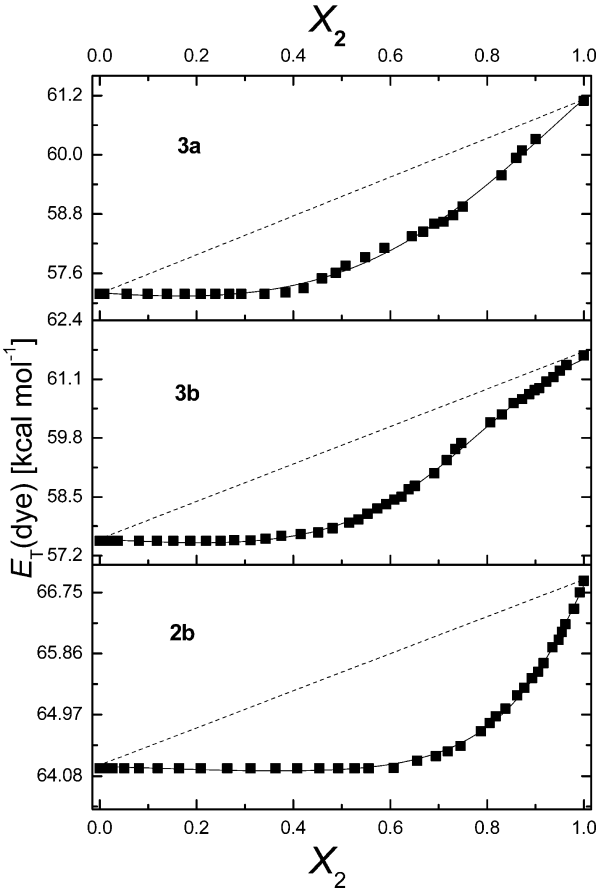

Figure 5. Influence of water on the E_T(dye) values of **3a–c** in methanol/water mixtures: (---) theoretical linear dependence for no PS; (—) curve fitted with eq 4; (■) experimental data.

solvated by the more polar moiety of the S_{12} species, while pyrene[13] and the dye 4-[4-(dimethylamino)styryl]-1-methylpyridinium iodide[20,27] are preferentially solvated by the less polar moiety of these complexes. For dyes **3a–c** in methanol/water mixtures, PS by the less polar moiety of S_{12} complexes occurs, as observed through the lower E_T values for the mixtures, which can be related to a less polar microenvironment.

Solvatochromic Switch Using 3d in Alcohol/Water Mixtures. Figure 6A shows a plot of the molar transition energies of **3d** as a function of the mole fraction of water, $X_2(H_2O)$, for water/methanol mixtures. A very unusual spectroscopic behavior occurs with this dye in these mixtures: the E_T(**3d**) value increases from 50.0 kcal mol^{-1} in pure methanol (a) to 52.7 kcal mol^{-1} after the addition of 80% (mol/mol) water (b). Subsequently, the addition of only another 5% (mol/mol) water causes a very sharp reduction in the E_T(**3d**) value to 39.1 kcal mol^{-1} (c), corresponding to a bathochromic shift from 543 to 732 nm ($\Delta\lambda$ = 189 nm). The subsequent addition of water leads to a mild reduction in the E_T(**3d**) value to finally 38.1 kcal mol^{-1} in pure water (d). The four selected UV–vis spectra presented in Figure 6B for this system show the spectral changes observed in the four regions of the system. The very large spectral shifts cause very different colors for solutions of **3d** in the solvent mixtures (see the inset in Figure 6A). This represents the first example of a solvatochromic switch triggered by a subtle change in the polarity of the medium, the color of the solutions being easily reversed by adding small amounts of the required cosolvent (Figure 6C).

To analyze the different solvation patterns of the observed trends in the electronic excitation of **3d**, molecular mechanics (MM) simulations were performed for this compound in different solvent environments, such as water, methanol, and two different methanol/water mixtures, with $X_2(H_2O)$ = 0.62 (i) and $X_2(H_2O)$ = 0.88 (ii), as shown in Figure 7. The two mixtures were chosen not only to investigate the drastic change in the absorption spectrum via the radial distribution function (RDF), but also to observe the difference in the solvation shells and the solute/solvent interactions in the system. The atoms chosen for the analysis were the phenolate oxygen atom in the donor moiety (named O25 in the MM simulations) and the nitro oxygen in the acceptor group (named O33). The representation of the solvent molecules in MM is depicted in Scheme 4. For the sake of clarity, only one nitro oxygen is considered in Figure 7, but all nitro oxygen atoms exhibit the same pattern. On analyzing the graphs, it is possible to observe distinct patterns for mixture i, which contains more methanol, and mixture ii, which is rich in water. The theoretical RDFs reveal that the solvation environment around the phenolate donor and nitro acceptor moieties, in particular for the first solvation shell, is distinct for each group depending on the solvent mixture employed. According to Figure 7, changes in the methanol concentration cause only minor variations in the RDFs for mixtures i and ii related to the nitro oxygen (Figure 7a,c). However, the same changes cause a considerable modification in the RDFs for the phenolate oxygen (Figure 7b,d). The RDFs make clear that, on increasing the methanol concentration, more hydrogen-bonding interactions between the methanol and phenolate groups are established, changing the solvent microenvironment of the dye and consequently modifying the absorption spectrum of compound **3d**.

Thus, the data show that in pure water **3d** is solvated through hydrogen bonding as shown in Scheme 3. With the addition of methanol to the medium, the alcohol molecules interact with water, forming S_{12} complexes and disrupting the HBs of the latter with the dye. The data suggest that the design of these S_{12} species enables them to interact with the 2,6-diphenylphenolate donor group of the dye, the less polar moiety of the species interacting via a hydrophobic effect, whereas the most polar moiety of the S_{12} species interacts with the oxygen atom of the donor group through hydrogen bonding. Therefore, the results suggest that the observed increase in the E_T(**3d**) values on

Table 2. Parameters of the Binary Methanol/Water Mixtures at 25 °C[a]

dye	$E_T(dye)_1$	$E_T(dye)_2$	$E_T(dye)_{12}$	$f_{2/1}$	$f_{12/1}$	$f_{12/2}$	SD
3a	64.2	66.9	63.5	0.0688	0.318	4.62	1.1×10^{-3}
3b	57.6	61.5	54.1	0.276	0.172	0.623	2.2×10^{-3}
3c	57.2	61.1	56.2	0.416	0.737	1.77	4.4×10^{-3}

[a]Calculated from eq 4 (see the text).

dx.doi.org/10.1021/jo301890r | J. Org. Chem. 2012, 77, 10668–10679

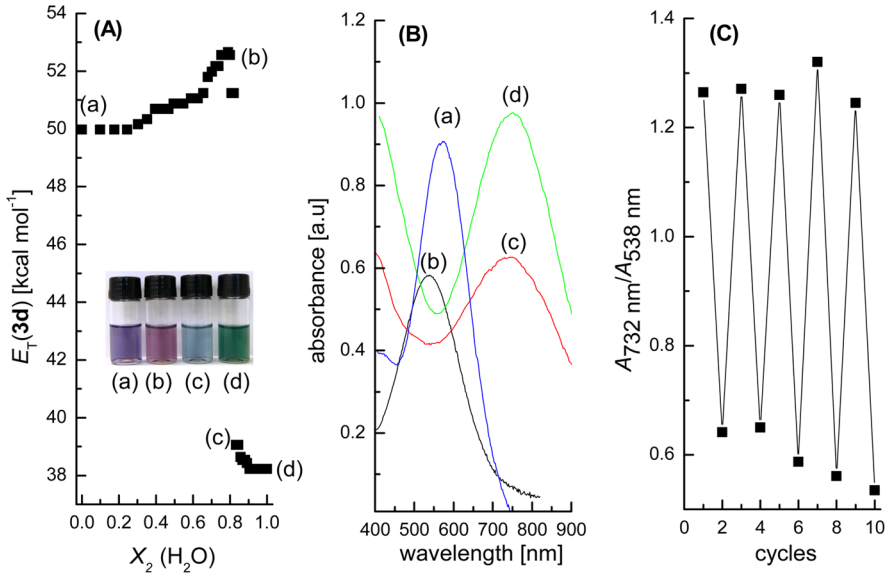

Figure 6. (A) Influence of water on the E_T(dye) values of **3d** in methanol/water mixtures: (■) experimental data. (B) Selected UV−vis spectra of **3d** in (a) pure methanol, (b) methanol with 80% (mol/mol) water, (c) methanol with 85% (mol/mol) water, and (d) pure water (the inset in (A) shows the corresponding solutions of **3d**). (C) Effect of the alternate addition of small volumes of methanol and water on the $A_{732\ nm}/A_{538\ nm}$ ratio in the region between 0.82 and 0.90.

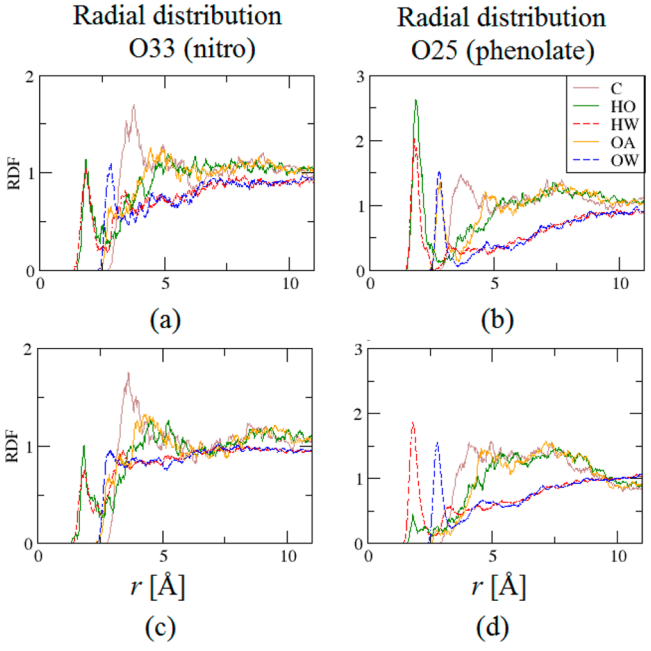

Figure 7. Radial distribution functions for methanol/water mixtures with $X_2(H_2O)$ = 0.62 (i) and $X_2(H_2O)$ = 0.88 (ii) for the nitro oxygen (named O33) and phenolate oxygen (named O25) atoms. (a) mixture i, atom O33; (b) mixture i, atom O25; (c) mixture ii, atom O33; (d) mixture ii, atom O25.

Scheme 4. Representation of the Solvent Molecules H_2O and H_3COH in the MM Simulations

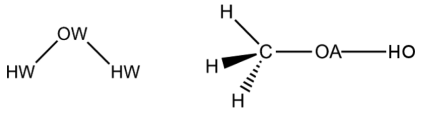

changing from pure methanol to 80% water reflects the PS of **3d** by the S_{12} species through these combined interactions. An analysis of the Kamlet−Taft parameters (Table 1) for the acidity and basicity of hydroxylic solvents shows that the α values decrease in the order water > methanol > ethanol > propan-1-ol, whereas the β values decrease in the reverse order. Thus, to verify whether solvent−solvent interactions are in fact responsible for the phenomenon observed, the spectroscopic behavior of **3d** was compared in mixtures of water with the three alcohols methanol (β = 0.66), ethanol (β = 0.75), and propan-1-ol (β = 0.90). Figure 8 shows plots of the molar

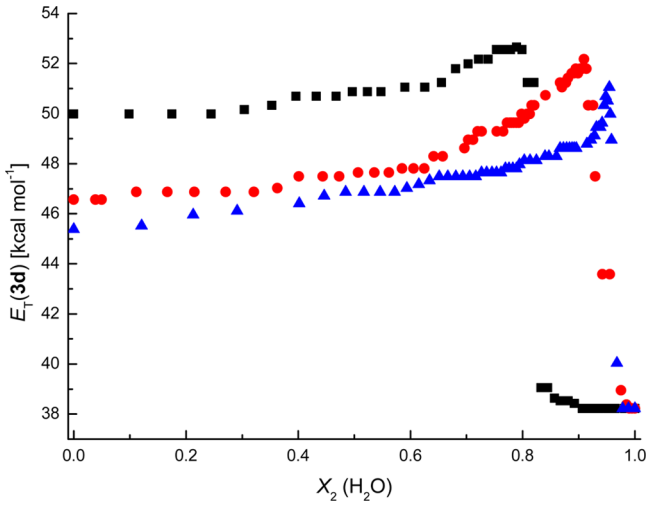

Figure 8. Variation in the E_T(**3d**) values according to binary mixtures of water with (■) methanol, (●) ethanol, and (▲) propan-1-ol.

transition energy values for the aqueous mixtures, where it can be observed that a change in the alcohol has a very important influence on the position of the maximum E_T(**3d**) value: methanol < ethanol < propan-1-ol, which corresponds to the increasing order of basicity of the alcohol. The more basic the alcohol, the stronger its interaction with water, causing the disruption of the HBs of the latter with the nitro groups of **3d**,

dx.doi.org/10.1021/jo301890r | J. Org. Chem. 2012, 77, 10668−10679

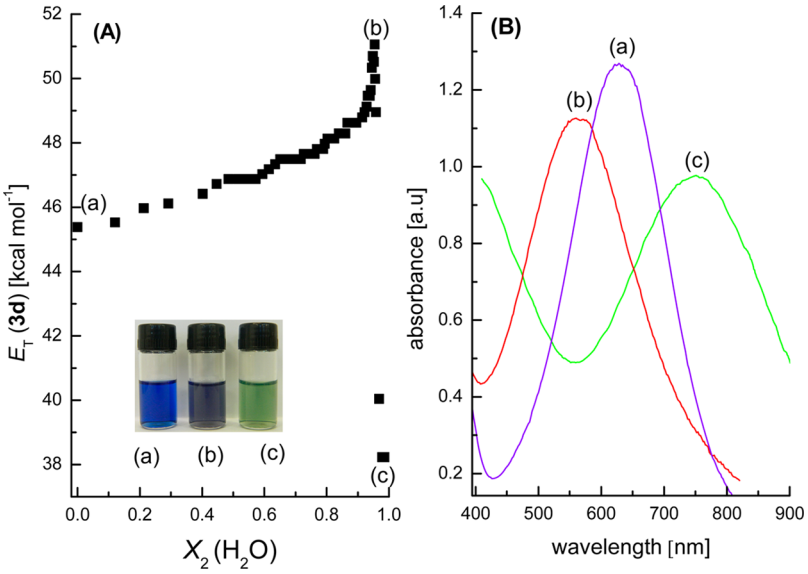

Figure 9. (A) Influence of water on the E_T(dye) values for **3d** in propan-1-ol/water mixtures. (B) Selected UV−vis spectra for **3d** in (a) propan-1-ol, (b) propan-1-ol with 96% (mol/mol) water, and (c) pure water. The inset in (A) shows the corresponding solutions of **3d**.

Table 3. Correlation Coefficients *a*, *b*, and *s* Obtained from the Catalán Multiparametric Analysis[a] through the Treatment of E_T(dye) Values for Compounds 3a−d in Various Solvents

dye	$E_T(dye)_0$	*a*	*b*	*s*	*N*	*F*	*r*	SD
3a	72.6 ± 4.6	15.2 ± 1.8	−2.4 ± 1.8	−21.1 ± 5.4	23	$<8 \times 10^{-7}$	0.89	2.3
3b	71.1 ± 5.2	16.3 ± 2.1	−6.1 ± 2.0	−25.2 ± 6.1	23	$<6 \times 10^{-7}$	0.89	2.6
3c	64.2 ± 3.2	18.6 ± 1.3	−3.4 ± 1.2	−18.5 ± 3.7	23	$<9 \times 10^{-11}$	0.96	1.6
3d	35.4 ± 8.0	19.9 ± 3.2	−2.6 ± 3.1	6.2 ± 9.3	23	$<3 \times 10^{-5}$	0.84	3.9

[a]Equation 7 was used (see the text).

and leading to the observed effects. Whereas in the methanol/water mixtures the E_T(**3d**) value has a maximum at 52.7 kcal mol^{-1} (80% water, mol/mol), in the ethanol mixtures (52.2 kcal mol^{-1}) this maximum occurs at 91% water (mol/mol), which leads to a band shift of $\Delta\lambda_{max}$ = 203.0 nm in comparison with the value for pure water.

A very impressive effect was observed for the propan-1-ol/water mixtures, as shown in Figure 9A. The addition of water to this alcohol leads to a hypsochromic shift of 70 nm up to E_T(**3d**) = 51.05 kcal mol^{-1} for a water mole fraction of 0.96. Above this value a strong decrease in the E_T(**3d**) value occurs. On the addition of only 4% (mol/mol) propan-1-ol to water, the λ_{max} shifts from 751.0 to 560.0 nm (Figure 9B), resulting in $\Delta\lambda_{max}$ = 191 nm, which can be monitored visually because the solution's change from green to violet (inset in Figure 9A).

Kamlet−Taft and Catalán Studies of the Solvatochromism of 3a−d. Two different analyses of the experimental E_T(dye) values in pure solvents for compounds **3a−d** were carried out with the use of the Kamlet−Taft[39,40,64−66] and Catalán[66−69] multiparameter approaches. These strategies consider a linear correlation between the measured spectroscopic parameter, E_T(dye), and several solvent parameters, as shown in the following equation:

$$E_T(\text{dye}) = E_T(\text{dye})_0 + aA + bB + cC + \ldots \quad (5)$$

where $E_T(dye)_0$ represents the E_T(dye) value relating to an inert solvent and *a*, *b*, and *c* are coefficients that reflect the importance of the solvent parameters *A*, *B*, and *C*, respectively, in terms of E_T(dye). The Kamlet−Taft strategy[39,40] makes use of the following equation:

$$E_T(\text{dye}) = E_T(\text{dye})_0 + a\alpha + b\beta + s(\pi^* + d\delta) \quad (6)$$

where δ is a polarizability correction term of the solvent. Another multiparametric polarity scale was developed by Catalán et al.,[67−69] which utilizes the following equation:

$$E_T(\text{dye}) = E_T(\text{dye})_0 + a(\text{SA}) + b(\text{SB}) + s(\text{SPP}) \quad (7)$$

where SPP, SA, and SB are parameters used to describe the solvent's dipolarity/polarizability, the HBD acidity, and the HBA basicity, respectively.

The contributions of the solvent properties to the E_T(dye) values obtained for **3a−d** were ascertained with the use of eqs 6 and 7, and the results of the multiple square correlation analysis are shown in Tables 3 and S2 and S3 (Supporting Information). A comparison between the data shows that, although the treatment with eq 6 gives reasonable SD and *r* values, the *b* values are very large and the *s* values are very small for dyes **3a−c**. These values are not consistent with the molecular structure of these dyes, which lack appreciably acidic sites to interact with the medium, and it is feasible to expect them to be appreciably sensitive to the dipolarity/polarizability of the solvent. The correlation analysis by means of the Catalán approach shows a more comprehensive picture for compounds **3a−c**, since the contribution of the HBA basicity of the solvent is small (small *b* coefficients), with very important contributions observed for the *a* (HBD acidity of the solvent) and *s* (dipolarity/polarizability) coefficients.

Figure 10 shows four plots that allow a comparison between the calculated and measured E_T(dye) values for **3c** and **3d** using the Kamlet−Taft and the Catalán parametrical analyses. These

dx.doi.org/10.1021/jo301890r | J. Org. Chem. 2012, 77, 10668−10679

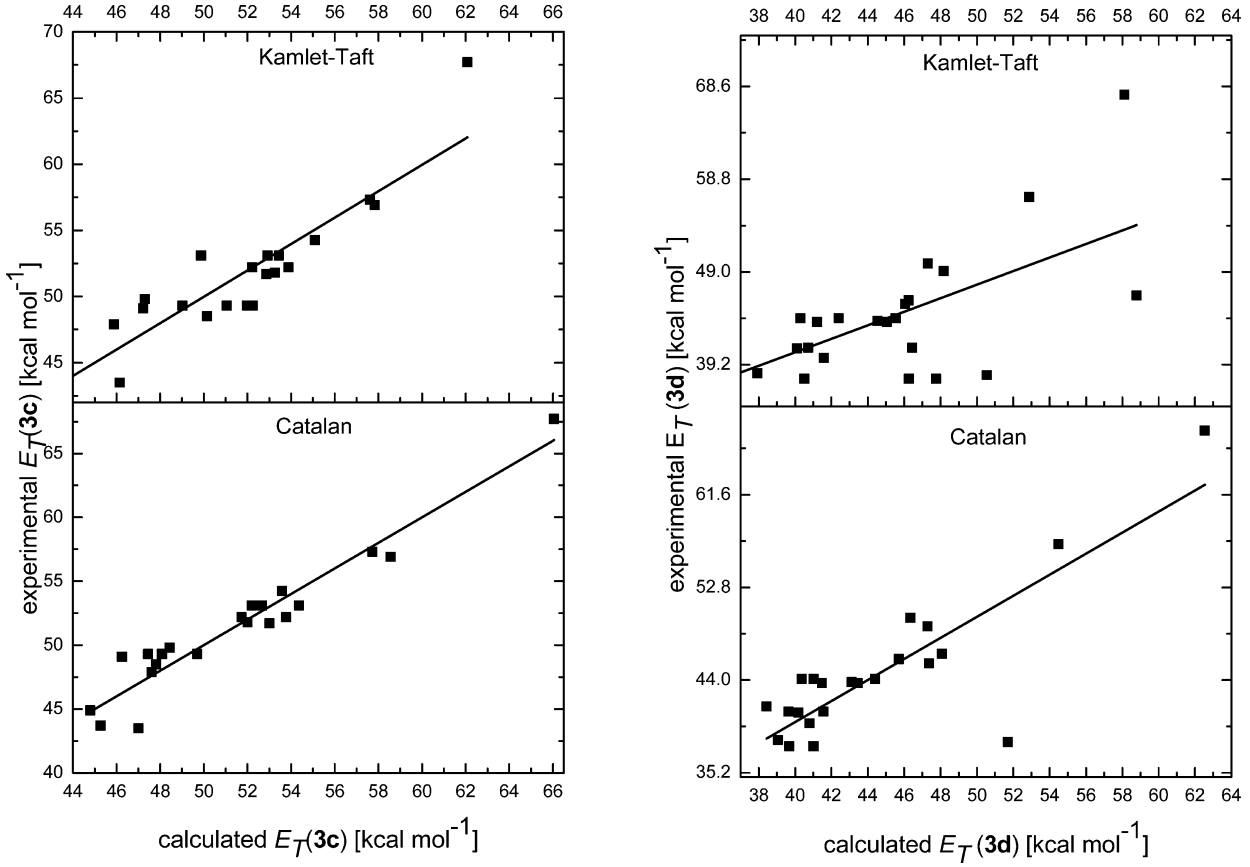

Figure 10. Relationships between calculated and measured E_T(dye) values for **3c** and **3d** in various solvents, considering the E_T(dye) values calculated using the Kamlet–Taft and Catalán approaches.

plots show that the Catalán parameters offer a better fitting of the data. For compound **3d** the *r* value obtained using the Catalán analysis is higher, but it is lower than those for the other compounds, and the *s* value is very different from those of the other dyes, suggesting a more complex solvation pattern. Following the procedure of El Seoud and co-workers,[65] and considering the fact that **3c** and **3d** have phenyl groups in their molecular structures, which would increase the lipophilicity of the dyes, an attempt was made to improve the correlations by adding, to the equations, the lipophilicity parameter log *P*. However, this parameter did not have any effect on the fittings. Thus, the results verify that the solvation of **3a–d** is mainly due to specific interactions through hydrogen bonding between the HB acceptor solvents and the nitro and/or the phenolate groups in the dyes combined with nonspecific solute–solvent interactions dictated by the dipolarity/polarizability of the solvents.

CONCLUSIONS

Dyes **3a–d** exhibit a very expressive solvatochromic behavior, with a reversal in solvatochromism observed for solvents with an $E_T(30)$ lower than ca. 43 kcal mol^{-1}. In addition, compound **3d** exhibits a remarkable behavior in hydroxylic solvents, since the E_T(**3d**) value increases with an increase in the $E_T(30)$ value of the alcohols, whereas in water an abrupt decrease occurs. The solvatochromism of the dyes is explained on the basis of the interaction of the dyes with the medium through combined solute/solvent effects, such as hydrogen bonding between the solvents and the nitro and phenolate groups and nonspecific solute/solvent interactions. Dye **3d** is specially tailored to be differently solvated in pure water or in the presence of small amounts of an alcoholic component, because in alcohol/water mixtures the two solvents interact with each other to form a third species (S_{12}) which is able to interact with the phenolate moiety. The MM simulations reinforce the observation that very small changes in the composition of the medium cause alterations in the microenvironment of the dye, leading to the modifications observed in its UV–vis absorption spectrum.

The synthesized compounds have the potential to be applied as probes in the investigation of binary solvent mixtures and other systems, such as surfactants in aqueous medium and the micropolarity of cyclodextrins, besides their possible applications as anionic chromogenic chemosensors.[38,70] In addition, the data presented herein indicate the possibility to synthesize *programmed* perichromic dyes (as shown by dye **3d**) that can be designed with stored information to be *read* by its solvation shell, which is translated into a sharp change in the optical signal with very subtle changes in the composition of the medium.[71] The authentic solvatochromic switch demonstrated by the behavior of **3d** in alcohol/water mixtures is of interest in relation to the synthesis of other systems, aimed at the design of smart materials that undergo changes in their optical properties, which are triggered by alterations in their microenvironment.

EXPERIMENTAL SECTION

Materials and Methods. All solvents were HPLC grade and were purified following the methodology described in the literature.[72,73] Deionized water was used in all measurements. It was boiled and

dx.doi.org/10.1021/jo301890r | J. Org. Chem. 2012, 77, 10668–10679

bubbled with nitrogen and kept in a nitrogen atmosphere to avoid the presence of carbon dioxide.

The melting points were uncorrected. The NMR spectra were recorded in DMSO-d_6 with a 400 MHz spectrometer. Chemical shifts were recorded in parts per million with the solvent resonance as the internal standard. Data are reported as follows: chemical shift, multiplicity (s = singlet, d = doublet, t = triplet), coupling constants (Hz), and integration. IR spectra were obtained with KBr pellets. Microanalyses are given as the average values of two determinations. High-resolution (HR) mass spectra were obtained with an electrospray ionization (ESI) quadrupole time-of-flight (QTOF) mass spectrometer.

Synthesis of the Compounds. Compound **2a** was synthesized by the reaction of 4-nitrobenzaldehyde with 4-aminophenol in ethanol at room temperature, and comparison of the characterization data with those in the literature[74] confirmed that **2a** was obtained.

Compound **2b** was prepared by means of the following procedure: 2,4-dinitrobenzaldehyde (0.100 g, 0.51 mmol), 4-aminophenol (0.055 g, 0.51 mmol), and methanol (10 mL) were added to an Erlenmeyer flask. The mixture was stirred until complete solubilization of the reactants. One drop of acetic acid was added, and the reaction mixture was stirred for 4 h. The mixture was left to stand in a freezer overnight. The precipitate formed was filtered off under vacuum, washed with iced methanol, and recrystallized three times from methanol. The product, after drying, was an amorphous yellow solid (0.079 g, yield 54%), with a melting point of 156.0−157.2 °C. IR (KBr, $\bar{\nu}_{max}$/cm^{-1}): 3460 (O−H), 1598 (C═N), 1439 (C═C), 1525, and 1342 (N═O). ^{1}H NMR (400 MHz, DMSO-d_6): δ/ppm 9.84 (1H, s) 8.92 (1H, s), 8.77 (1H, s), 8.60 (1H, d, J = 8.4 Hz), 8.40 (1H, d, J = 8.4 Hz), 7.31 (2H, d, J = 7.8 Hz), 6.85 (2H, d, J = 7.8 Hz). ^{13}C NMR (100 MHz, DMSO-d_6): δ/ppm 158.4, 151.2, 149.1, 148.2, 141.6, 135.8, 131.2, 128.1, 124.0, 120.6, 116.4. Anal. Calcd for $C_{13}H_9N_3O_5$: C, 54.36; H, 3.16; N, 14.63. Found: C, 54.33; H, 3.18; N, 14.61. HRMS (ESI, TOF): m/z calcd for $C_{13}H_{10}N_3O_5$ $[M + H]^+$ 288.0620, found 288.0615.

For the synthesis of compounds **2c** and **2d**, 4-amino-2,6-diphenylphenol was obtained according to the procedure described in the literature:[75] 2,6-diphenylphenol was stirred with an excess of sodium nitrite, followed by reduction of the product with granulated tin and concentrated HCl.

Compound **2c** was prepared by means of a procedure described recently.[38]

Compound **2d** was prepared by a procedure similar to that described for **2b**, but using ethanol (5 mL) as the solvent, as well as 2,4-dinitrobenzaldehyde (0.100 g, 0.51 mmol) and 4-amino-2,6-diphenylphenol (0.133 g, 0.51 mmol). The precipitate formed after freezing overnight was filtered off under vacuum, washed with iced ethanol, and recrystallized three times from ethanol. The dried product was an amorphous orange solid (0.094 g, yield 42%), with a melting point of 126.1−126.9 °C. IR (KBr, $\bar{\nu}_{max}$/cm^{-1}): 3438 (O−H), 1598 (C═N), 1463, 1427 (C═C), 1524, 1346 (N═O), and 1226 (C−O). ^{1}H NMR (400 MHz, DMSO-d_6): δ/ppm 9.07 (1H, s) 8.79 (1H, d, J = 2.4 Hz), 8.71 (1H, s), 8.63 (1H, dd, J = 8.6 and 2.4 Hz), 8.42 (1H, d, J = 8.6 Hz), 7.61 (4H, d, J = 8.4 Hz), 7.49 (4H, t, J = 7.6 Hz), 7.39 (2H, t, J = 7.6 Hz), 7.31 (2H, s). ^{13}C NMR (100 MHz, DMSO-d_6): δ/ppm 150.5, 150.0, 148.9, 148.3, 142.7, 136.7, 136.1, 131.1, 129.8, 129.3, 129.0, 128.2, 127.4, 123.5, 120.4. Anal. Calcd for $C_{25}H_{17}N_3O_5$: C, 68.33; H, 3.90; N, 9.56. Found: C, 68.56; H, 3.92; N, 9.54. HRMS (ESI, TOF): m/z calcd for $C_{25}H_{18}N_3O_5$ $[M + H]^+$ 440.1246, found 440.1278.

UV−Vis Measurements. The following procedure was typical for all measurements performed. A 1.0×10^{-2} mol L^{-1} stock solution of compounds **2a−d** was prepared in anhydrous dichloromethane. From this stock solution 5 μL was transferred to two 5 mL volumetric flasks. After evaporation of the dichloromethane the probe was dissolved in the pure solvent, resulting in a solution presenting a final dye concentration of 1.0×10^{-5} mol L^{-1}. To generate the deprotonated compounds **3a−d**, 2 μL of a 0.2 mol L^{-1} tetra-*n*-butylammonium hydroxide aqueous solution was added to each flask. This very small amount of added water did not shift the UV−vis band of the dye. The bulky tetra-*n*-butylammonium ion has no influence on the UV−vis spectrum of the anionic dye. The UV−vis spectra were recorded at 25 °C, using a 1 cm square cuvette. The maxima of the UV−vis spectra were calculated from the first derivative of the absorption spectrum. The λ_{max} values thus obtained were transformed into E_T(dye) values, according to the expression E_T(dye) = 28590/λ_{max}.[1,5]

Mixed Solvents. Binary mixtures were prepared by weighing, in a quartz cuvette, the solutions of each dye prepared as described above, and the final values are expressed in terms of the mole fraction X_2. The cuvette was kept hermetically closed with a rubber stopper to minimize problems with solvent evaporation. The maxima of the emission spectra were determined, and the λ_{max} values thus obtained were transformed into E_T(dye) values (see above). All experiments with the mixed solvent systems were carried out in duplicate, and the reproducibility of the curve features was confirmed.

Computational Details. The structural and electronic properties of the dyes were calculated with the Gaussian 03 package,[76] using the DFT level of theory, with the B3LYP[77−80] functional and 6-31G** basis set.[81,82] All calculated molecular structures correspond to a minimum on the potential energy surface, since no imaginary values were obtained in the Hessian matrix. The MM simulations were obtained via the GROMACS package,[83] using the OPLS-AA[84,85] force field and the water model SPC/E.[86] Simulation boxes containing the pure solvents (water and ethanol) and mixtures (mixture i, X_2 = 0.62; mixture ii, X_2 = 0.88), containing approximately 780 solvent molecules, were thermalized at the NVT ensemble (temperature 298 K, τ = 0.1 ps) for 500 ps and equilibrated at the NPT ensemble (pressure 1 bar, τ_P = 0.2 ps) for 2 ns. To describe the anionic compound **3d** via the MM method, the molecular structure of compound **2d** was used as the basis and the charges for the molecule were obtained via the CHelpG method,[87] using the Gaussian 03 program.[76]

Calculation Methods. The parameters $E_T(dye)_1$, $E_T(dye)_2$, $E_T(dye)_{12}$, $f_{2/1}$, and $f_{12/1}$ in the studies of the solvent mixtures containing **2b−4b** were calculated, and the multiparametric analysis was performed from nonlinear regressions using ORIGIN 8.5 software.

■ ASSOCIATED CONTENT

Ⓢ Supporting Information

IR, LRMS, HRMS, and ^{1}H and ^{13}C NMR data for compounds **2b** and **2d**, experiments used to discard aggregation of **3d**, UV−vis spectra of **3d** in water and methanol, "polarity" parameters for the pure solvents, tables containing the correlation coefficients obtained from the multiparametric analyses, correlation of experimental and calculated E_T values for **3a** and **3b**, and tables of atom coordinates and absolute energies for compounds **2d** and **3d**. This material is available free of charge via the Internet at http://pubs.acs.org.

■ AUTHOR INFORMATION

Corresponding Author

*E-mail: vanderlei.machado@ufsc.br.

Notes

The authors declare no competing financial interest.

■ ACKNOWLEDGMENTS

Financial support of the Brazilian Conselho Nacional de Desenvolvimento Científico e Tecnológico (CNPq), Coordenação de Aperfeiçoamento de Pessoal de Nível Superior (Capes), and UFSC is gratefully acknowledged.

■ REFERENCES

(1) Reichardt, C.; Welton, T. *Solvents and Solvent Effects in Organic Chemistry*, 4th ed.; Wiley-VCH: Weinheim, Germany, 2010; Chapters 6 and 7.

(2) Suppan, P.; Ghoneim, N. *Solvatochromism*, 1st ed.; Royal Society of Chemistry: Cambridge, U.K., 1997; Chapter 3.

(3) Bagno, A. *J. Phys. Org. Chem.* **2002**, *15*, 790−795.
(4) El Seoud, O. A. *Pure Appl. Chem.* **2009**, *81*, 697−707.
(5) Reichardt, C. *Chem. Rev.* **1994**, *94*, 2319−2358.
(6) Reichardt, C. *Pure Appl. Chem.* **2008**, *80*, 1415−1432.
(7) Dimroth, K.; Reichardt, C. *Fresenius' Z. Anal. Chem.* **1966**, *215*, 344−350.
(8) Marcus, Y. *J. Chem. Soc., Perkin Trans. 2* **1994**, 1015−1021.
(9) Marcus, Y. *J. Chem. Soc., Faraday Trans.* **1995**, *91*, 427−430.
(10) Catalán, J.; Díaz, C.; García-Blanco, F. *J. Org. Chem.* **2000**, *65*, 9226−9229.
(11) Ghoneim, N. *Spectrochim. Acta, Part A* **2001**, *57*, 1877−1884.
(12) Leitão, R. E.; Martins, F.; Ventura, M. C.; Nunes, N. *J. Phys. Org. Chem.* **2002**, *15*, 623−630.
(13) Silva, M. A. do R.; da Silva, D. C.; Machado, V. G.; Longhinotti, E.; Frescura, V. L. A. *J. Phys. Chem. A* **2002**, *106*, 8820−8826.
(14) da Silva, D. C.; Ricken, I.; Silva, M. A. d. R.; Machado, V. G. *J. Phys. Org. Chem.* **2002**, *15*, 420−427.
(15) Herodes, K.; Koppel, J.; Reichardt, C.; Koppel, I. A. *J. Phys. Org. Chem.* **2003**, *16*, 626−632.
(16) Bae, S. Y.; Arnold, B. R. *J. Phys. Org. Chem.* **2004**, *17*, 187−193.
(17) Bevilaqua, T.; da Silva, D. C.; Machado, V. G. *Spectrochim. Acta, Part A* **2004**, *60*, 951−958.
(18) Martins, C. T.; Lima, M. S.; El Seoud, O. A. *J. Phys. Org. Chem.* **2005**, *18*, 1072−1085.
(19) Cavalli, V.; da Silva, D. C.; Machado, C.; Machado, V. G.; Soldi, V. *J. Fluoresc.* **2006**, *16*, 77−86.
(20) Bevilaqua, T.; Gonçalves, T. F.; Venturini, C. de G.; Machado, V. G. *Spectrochim. Acta, Part A* **2006**, *65*, 535−542.
(21) Keum, S. R.; Roh, S. J.; Ahn, S. M.; Lim, S. S.; Kim, S. H.; Koh, K. *Dyes Pigm.* **2007**, *74*, 343−347.
(22) Mellein, B. R.; Aki, S. N. V. K.; Ladewski, R. L.; Brennecke, J. F. *J. Phys. Chem. B* **2007**, *111*, 131−138.
(23) Moita, M. L.; Teodoro, R. A.; Pinheiro, L. M. *J. Mol. Liq.* **2007**, *136*, 15−21.
(24) Sarkar, A.; Trivedi, S.; Baker, G. A.; Pandey, S. *J. Phys. Chem. B* **2008**, *112*, 14927−14936.
(25) Umadevi, M.; Vanelle, P.; Terme, T.; Rajkumar, B. J. M.; Ramakrishnan, V. *J. Fluoresc.* **2008**, *18*, 1139−1149.
(26) Marcus, Y. *J. Mol. Liq.* **2008**, *140*, 61−67.
(27) Testoni, F. M.; Ribeiro, E. A.; Giusti, L. A.; Machado, V. G. *Spectrochim. Acta, Part A* **2009**, *71*, 1704−1711.
(28) Giusti, L. A.; Marini, V. G.; Machado, V. G. *J. Mol. Liq.* **2009**, *150*, 9−15.
(29) Sato, B. M.; de Oliveira, C. G.; Martins, C. T.; El Seoud, O. A. *Phys. Chem. Chem. Phys.* **2010**, *12*, 1764−1771.
(30) Farajtabar, A.; Jaberi, F.; Gharib, F. *Spectrochim. Acta, Part A* **2011**, *83*, 213−220.
(31) Panigrahi, M.; Dash, S.; Patel, S.; Mishra, B. K. *J. Phys. Chem. B* **2011**, *115*, 99−108.
(32) Adegoke, O. A. *Spectrochim. Acta, Part A* **2011**, *83*, 504−510.
(33) Khupse, N. D.; Kumar, A. *J. Phys. Chem. B* **2011**, *115*, 711−718.
(34) Patel, S.; Sukhamoy, G.; Kumar, M. P. *J. Photochem. Photobiol., A* **2011**, *219*, 76−83.
(35) Sarkar, A.; Kedia, N.; Purkayastha, P.; Bagchi, S. *J. Lumin.* **2011**, *131*, 1731−1738.
(36) Krygowski, T. M.; Wrona, P. K.; Zielkowska, U.; Reichardt, C. *Tetrahedron* **1985**, *41*, 4519−4527.
(37) Kijevcanin, M. L.; Djuris, M. M.; Radovic, I. R.; Djordjevic, B. D.; Serbanovic, S. P. *J. Chem. Eng. Data* **2007**, *52*, 1136−1140.
(38) Marini, V. G.; Zimmermann, L. M.; Torri, E.; Machado, V. G. *ARKIVOC* **2010**, *xi*, 146−162.
(39) Kamlet, M. J.; Abboud, J.-L. M.; Abraham, M. H.; Taft, R. W. *J. Org. Chem.* **1983**, *48*, 2877−2887.
(40) Marcus, Y. *Chem. Soc. Rev.* **1993**, *22*, 409−416.
(41) Benson, H. G.; Murrell, J. N. *J. Chem. Soc., Faraday Trans. 2* **1972**, *68*, 137−143.
(42) da Silva, L.; Machado, C.; Rezende, M. C. *J. Chem. Soc., Perkin Trans. 2* **1995**, 483−488.
(43) Mishra, B. K.; Kuanar, M.; Mishra, A.; Behera, G. B. *Bull. Chem. Soc. Jpn.* **1996**, *69*, 2581−2584.
(44) Aliaga, C.; Galdames, J. S.; Rezende, M. C. *J. Chem. Soc., Perkin Trans. 2* **1997**, 1055−1058.
(45) Panigrahi, M.; Dash, S.; Patel, S.; Behera, P. K.; Mishra, B. K. *Spectrochim. Acta, Part A* **2007**, *68*, 757−762.
(46) Martins, C. T.; Lima, M. S.; Bastos, E. L.; El Seoud, O. A. *Eur. J. Org. Chem.* **2008**, 1165−1180.
(47) Murugan, N. A.; Kongsted, J.; Rinkevicius, Z. *Phys. Chem. Chem. Phys.* **2011**, *13*, 1290−1292.
(48) Dominguez, M.; Rezende, M. C. *J. Phys. Org. Chem.* **2010**, *23*, 156−170.
(49) Niedbalska, M.; Gruda, I. *Can. J. Chem.* **1990**, *68*, 691−695.
(50) Catalán, J.; Mena, E.; Meutermans, W.; Elguero, J. *J. Phys. Chem.* **1992**, *96*, 3615−3621.
(51) Tsukada, M.; Mineo, Y.; Itoh, K. *J. Phys. Chem.* **1989**, *93*, 7989−7992.
(52) Hisamoto, H.; Tohma, H.; Yamada, T.; Yamauchi, K.; Siswanta, D.; Yoshioka, N.; Suzuki, K. *Anal. Chim. Acta* **1998**, *373*, 271−289.
(53) Marcus, Y. *J. Solution Chem.* **1991**, *20*, 929−944.
(54) Zhao, G.-J.; Han, K.-L. *Acc. Chem. Res.* **2012**, *45*, 404−413.
(55) Zhao, G.-J.; Liu, J.-Y.; Zhou, L.-C.; Han, K.-L. *J. Phys. Chem. B* **2007**, *111*, 8940−8945.
(56) Zhao, G.-J.; Han, K.-L. *Biophys. J.* **2008**, *94*, 38−46.
(57) Skwierczynski, R. D.; Connors, K. A. *J. Chem. Soc., Perkin Trans. 2* **1994**, 467−472.
(58) Rosés, M.; Ràfols, C.; Ortega, J.; Bosch, E. *J. Chem. Soc., Perkin Trans. 2* **1995**, 1607−1615.
(59) Bosch, E.; Rosés, M.; Herodes, K.; Koppel, I.; Leito, I.; Koppel, I.; Taal, V. *J. Phys. Org. Chem.* **1996**, *9*, 403−410.
(60) Herodes, K.; Leito, I.; Koppel, I.; Rosés, M. *J. Phys. Org. Chem.* **1999**, *12*, 109−115.
(61) Maksimović, Z. B.; Reichardt, C.; Spirić, A. *Fresenius' Z. Anal. Chem.* **1974**, *270*, 100−104.
(62) Machado, V. G.; Machado, C.; Nascimento, M. da G.; Rezende, M. C. *J. Phys. Org. Chem.* **1997**, *10*, 731−736.
(63) Fayed, T.; Etaiw, S. E. H. *Spectrochim. Acta, Part A* **1998**, *54*, 1909−1918.
(64) El-Sayed, M.; Muller, H.; Rheinwald, G.; Lang, H.; Spange, S. *Chem. Mater.* **2003**, *15*, 746−754.
(65) Martins, C. T.; Lima, M. S.; El Seoud, O. A. *J. Org. Chem.* **2006**, *71*, 9068−9079.
(66) Jayabharathi, J.; Thanikachalam, V.; Devi, K. B.; Perumal, M. V. *J. Fluoresc.* **2012**, *22*, 737−744.
(67) Catalán, J.; López, V.; Pérez, P.; Martín-Villamil, R.; Rodriguez, J.-G. *Liebigs Ann.* **1995**, 241−252.
(68) Catalán, J.; López, V.; Pérez, P. *Liebigs Ann.* **1995**, 793−795.
(69) Catalán, J.; Díaz, C.; López, V.; Pérez, P.; de Paz, J.-L. G.; Rodriguez, J.-G. *Liebigs Ann.* **1996**, 1785−1794.
(70) Nicoleti, C. R.; Marini, V. G.; Zimmermann, L. M.; Machado, V. G. *J. Braz. Chem. Soc.* **2012**, *23*, 1488−1500.
(71) de Silva, A. P.; McClenaghan, N. D. *Chem.—Eur. J.* **2004**, *10*, 574−586.
(72) Furniss, B. S.; Hannaford, A. J.; Smith, P. W. G.; Tatchell, A. R. *Vogel's Textbook of Practical Organic Chemistry*, 5th ed.; Longman: London, 1989.
(73) Williams, D. B. G.; Lawton, M. *J. Org. Chem.* **2010**, *75*, 8351−8354.
(74) Kaya, I.; Culhaoglu, S. *Iran. Polym. J.* **2006**, *15*, 487−495.
(75) Rezende, M. C.; Radetski, C. M. *Quim. Nova* **1988**, *11*, 353−354; *Chem. Abstr.* **1989**, *111*, 8876w.
(76) Frisch, M. J.; Trucks, G. W.; Schlegel, H. B.; Scuseria, G. E.; Robb, M. A.; Cheeseman, J. R.; Montgomery, J. A., Jr.; Vreven, T.; Kudin, K. N.; Burant, J. C.; Millam, J. M.; Iyengar, S. S.; Tomasi, J.; Barone, V.; Mennucci, B.; Cossi, M.; Scalmani, G.; Rega, N.; Petersson, G. A.; Nakatsuji, H.; Hada, M.; Ehara, M.; Toyota, K.; Fukuda, R.; Hasegawa, J.; Ishida, M.; Nakajima, T.; Honda, Y.; Kitao, O.; Nakai, H.; Klene, M.; Li, X.; Knox, J. E.; Hratchian, H. P.; Cross, J. B.; Bakken, V.; Adamo, C.; Jaramillo, J.; Gomperts, R.; Stratmann, R.

E.; Yazyev, O.; Austin, A. J.; Cammi, R.; Pomelli, C.; Ochterski, J. W.; Ayala, P. Y.; Morokuma, K.; Voth, G. A.; Salvador, P.; Dannenberg, J. J.; Zakrzewski, V. G.; Dapprich, S.; Daniels, A. D.; Strain, M. C.; Farkas, O.; Malick, D. K.; Rabuck, A. D.; Raghavachari, K.; Foresman, J. B.; Ortiz, J. V.; Cui, Q.; Baboul, A. G.; Clifford, S.; Cioslowski, J.; Stefanov, B. B.; Liu, G.; Liashenko, A.; Piskorz, P.; Komaromi, I.; Martin, R. L.; Fox, D. J.; Keith, T.; Al-Laham, M. A.; Peng, C. Y.; Nanayakkara, A.; Challacombe, M.; Gill, P. M. W.; Johnson, B.; Chen, W.; Wong, M. W.; Gonzalez, C.; Pople, J. A. *Gaussian 03*, revision C02; Gaussian Inc.: Wallingford, CT, 2004.

(77) Becke, A. D. *J. Chem. Phys.* **1993**, *98*, 5648−5652.

(78) Lee, C.; Yang, W.; Parr, R. G. *Phys. Rev. B* **1988**, *37*, 785−789.

(79) Vosko, S. H.; Wilk, L.; Nusair, M. *Can. J. Phys.* **1980**, *58*, 1200−1211.

(80) Stephens, P. J.; Devlin, F. J.; Chabalowski, C. F.; Frisch, M. J. *J. Phys. Chem.* **1994**, *98*, 11623−11627.

(81) Rassolov, V. A.; Pople, J. A.; Ratner, M. A.; Windus, T. L. *J. Chem. Phys.* **1998**, *109*, 1223−1229.

(82) Rassolov, V. A.; Ratner, M. A.; Pople, J. A.; Redfern, P. C.; Curtiss, L. A. *J. Comput. Chem.* **2001**, *22*, 976−984.

(83) Hess, B.; Kutzner, C.; van der Spoel, D.; Lindahl, E. *J. Chem. Theory Comput.* **2008**, *4*, 435−447.

(84) Jorgensen, W. L.; Tirado-Rives, J. *J. Am. Chem. Soc.* **1988**, *6*, 1657−1666.

(85) Jorgensen, W. L; Maxwell, D. S.; Tirado-Rives, J. *J. Am. Chem. Soc.* **1996**, *118*, 11225−11236.

(86) Berendsen, H. J. C.; Grigera, J. R.; Straatsma, T. P. *J. Phys. Chem.* **1987**, *91*, 6269−6271.

(87) Breneman, C. M.; Wiberg, K. B. *J. Comput. Chem.* **1990**, *11*, 361−373.